DOI: https://doi.org/10.17816/0321-4443-628957
Original Study Article

Estimation of influence of ride smoothness of transport-technological machines on driving safety in off-road conditions

Roman R. Bukirov

St. Petersburg State University of Architecture and Civil Engineering, Saint Petersburg, Russian Federation

ABSTRACT

BACKGROUND: Driving safety of transport-technological machines, especially in off-road conditions, largely depends on the stiffness and damping of suspension. These properties directly affect the ride smoothness and static transverse stability of the vehicle on a slope, ensure the ability of long-term motion on rough roads in the range of operating velocities without exceeding the established limits of vibration accelerations, causing unpleasant sensations and rapid fatigue of a driver, constant contact of wheels with the ground, as well as avoiding excessive wheel bump. Therefore, it is necessary to provide the suspension with the required elastic and damping characteristics by using a pneumohydraulic shock absorber in the design and to evaluate its effect on the safety of driving in off-road conditions.

AIM: The work aimed to develop a method for assessing the impact of ride smoothness of transport and technological machines on the main indicators of driving safety in off-road conditions in the development of new technical solutions aimed at improving the ride smoothness.

METHODS: The work employed modeling of oscillatory processes of the vehicle masses connected with each other by stiffness-damping links at unsteady and steady oscillations, modeling of the influence of the stiffness of the elastic suspension element on the static transverse stability of the vehicle on a slope are performed in the Mathcad software environment.

RESULTS: The mathematical modeling of oscillatory processes of masses of the vehicle resulted in establishment that the application of the proposed shock absorber enables in case of driving over a single bump of 0.08 m height at a speed of 30 km/h to reduce body displacement from 0.070 m to 0.056 m and its acceleration from 3.50 m/s^2 to 1.35 m/s^2, there by achieving complete damping of the oscillatory process of the masses already in the period 4, and in the case of driving over a sinusoidal bump, the oscillatory process is largely stabilized, the wheel follows the bump profile, and as a result the body movement decreases from 0.045 m to 0.030 m, and the acceleration of the body after the transition process decreases from 2.2 m/s^2 to 0.8 m/s^2. The analysis of evaluation of influence of smooth running on static transverse stability of the vehicle has shown that as a result of considering the elastic and hydraulic characteristics of the shock absorber and the pneumatic tires themselves, the angle of static stability on lateral overturning can be increased from 38° to 43° with maximum permissible angle of body roll of 8.4°.

CONCLUSION: The knowledge of methods of estimation of influence of ride smoothness of transport-technological machines on the main indicators of driving safety in off-road conditions enables to analyze the efficiency of application of the proposed technical solutions aimed at increasing the ride smoothness of the vehicle in off-road conditions.

Keywords: transport-technological machines; vehicle suspension; pneumohydraulic shock absorber; oscillating system of suspension; elastic-damping property of suspension; static transverse stability of vehicle.

To cite this article:
Bukirov RR. Estimation of influence of ride smoothness of transport-technological machines on driving safety in off-road conditions *Tractors and Agricultural Machinery.* 2024;91(5):619–636. DOI: https://doi.org/10.17816/0321-4443-628957

Received: 11.03.2024 **Accepted:** 26.11.2024 **Published online:** 03.12.2024

DOI: https://doi.org/10.17816/0321-4443-628957

Оригинальное исследование

Оценка влияния плавности хода транспортно-технологических машин на безопасность движения в условиях бездорожья

Р.Р. Букиров

Санкт-Петербургский государственный архитектурно-строительный университет (СПбГАСУ), Санкт-Петербург, Российская Федерация

АННОТАЦИЯ

Обоснование. Безопасность движения транспортно-технологических машин, особенно в условиях бездорожья, в значительной степени зависит от упругодемпфирующих свойств подвески, которые непосредственно влияют на плавность хода и статическую поперечную устойчивость машины на косогоре, обеспечивают возможность длительного движения по неровным дорогам в интервале эксплуатационных скоростей без превышения установленных норм виброускорений, вызывающих неприятные ощущения и быструю утомляемость у водителя, безотрывного движения колеса от дороги, а также «непробоя» подвески. Поэтому для подвески необходимо обеспечить требуемые упругодемпфирующие характеристики путем применения в конструкции пневмогидравлического амортизатора и провести оценку его влияния на безопасность движения в условиях бездорожья.

Цель работы — разработка метода оценки влияния плавности хода транспортно-технологических машин на главные показатели безопасности движения в условиях бездорожья при разработке новых технических решений, направленных на повышение плавности хода.

Методы. Моделирование колебательных процессов масс машины, соединённых между собой упругодемпфирующими связями при неустановившихся и установившихся колебаниях, моделирование влияние жёсткости упругого элемента подвески на статическую поперечную устойчивость машины на косогоре, выполненных в программной среде Mathcad.

Результаты. В результате математического моделирования колебательных процессов масс машины было установлено, что применение предлагаемого амортизатора позволяет в случае проезда единичной неровности высотой 0,08 м при скорости движения машины в 30 км/ч снизить перемещения кузова с 0,070 м до 0,056 м и его ускорения с 3,50 м/с^2 до 1,35 м/с^2, тем самым достигается полное гашение колебательного процесса масс уже в четвертом периоде, а в случае движения по синусоидальной неровности колебательный процесс в значительной степени стабилизируется, колесо копирует профиль неровности, в результате чего перемещение кузова снижается с 0,045 м до 0,030 м, а ускорение кузова после переходного процесса снижается с 2,2 м/с^2 до 0,8 м/с^2. Анализ оценки влияния плавности хода на статическую поперечную устойчивость машины показал, что в результате учета упругодемпфирующих характеристик амортизатора и самих пневмошин позволяет повысить угол статической устойчивости по боковому опрокидыванию с 38 до 43 при максимально допустимом угле крена кузова в 8,4.

Заключение. Знание методик оценки влияния плавности хода транспортно-технологических машин на главные показатели безопасности движения в условиях бездорожья позволяют провести анализ эффективности применения предлагаемых технических решений, направленных на повышение плавности хода машины в условиях бездорожья.

Ключевые слова: транспортно-технологические машины; подвеска машины; пневмогидравлический амортизатор; колебательная система подвески; упругодемпфирующая характеристика подвески; статическая поперечная устойчивость машины.

Как цитировать:
Букиров Р.Р. Оценка влияния плавности хода транспортно-технологических машин на безопасность движения в условиях бездорожья // Тракторы и сельхозмашины. 2024. Т. 91, № 5. С. 619–636. DOI: https://doi.org/10.17816/0321-4443-628957

Рукопись получена: 11.03.2024 **Рукопись одобрена:** 26.11.2024 **Опубликована online:** 03.12.2024

INTRODUCTION

The safety of transport and technological machines (TTMs) based on the truck chassis with a high center of gravity in off-road conditions largely depends on the elastic-damping properties of the suspension. The design and characteristics of these systems determine the reliability of wheel contact with the ground when driving over uneven terrain [1–10] and the vehicle's stability on rough roads [11–19].

Oscillations of the vehicle's sprung and unsprung masses caused by uneven surfaces negatively impact key traffic safety parameters, especially in off-road conditions. Both the suspension system and pneumatic tires are designed to minimize these oscillations [20]. Their combined performance significantly affects ride smoothness and, consequently, overall driving safety. Mass oscillations largely depend on the vehicle parameters and their relationships. These parameters include [9, 10, 21] the masses of the sprung and unsprung parts, suspension damping levels, suspension rigidity, and pneumatic tire rigidity. Changes to these parameters greatly affect the oscillatory processes. Typically, simple single-mass oscillatory systems are used to evaluate how the damping oscillations of the sprung mass are dampened under different system parameters. However, these models do not account for the influence of unsprung masses, which are critical to understanding the stability of the vehicle and its contact with the road [20]. To study the oscillatory process of all vehicle masses, a two-mass oscillatory system is used [6, 20]. This model incorporates the effects of unsprung masses in the vehicle oscillatory system. It enables a more detailed evaluation of how these unsprung masses influence the oscillations of sprung masses, vehicle stability, and the consistent contact of wheels with the ground.

PROBLEM STATEMENT

A previous study [4] proposed a technical solution involving a pneumohydraulic shock absorber (PHS) containing an elastic element in the form of an internal pneumatic chamber [22]. Single-mass oscillatory systems were adopted as oscillatory systems. Free oscillations arising after the vehicle body is raised and dropped from a certain height were analyzed to simulate the effects of driving over uneven terrain. However, since vehicle motion on uneven roads typically generates unsteady oscillations, followed by free oscillations after passing such surfaces [10], a more realistic understanding of the vehicle's oscillatory behavior was needed. This study focuses on both unsteady and steady oscillations of a vehicle using two-mass oscillatory systems that were implemented in the Mathcad software environment. A patented technical solution, featuring a PHS design with an additional pneumatic chamber, is examined. Particular attention is paid to evaluating the effect of the elastic element of the proposed PHS and pneumatic tires on the static lateral stability of the vehicle. The research was conducted on a TTM based on the chassis of a KAMAZ 43502 truck. This TTM is equipped with repair tools intended for the maintenance of other TTMs located at construction sites far from established road infrastructure.

ANALYSIS OF ROAD IRREGULARITIES UNDER OFF-ROAD CONDITIONS

Road irregularities, characterized by conditions like potholes, subsidence, distorted cross-sections, and alternating transverse ridges and depressions with slightly sloping edges, are registered. These uneven surfaces severely impact the suspension system and exert increased stress on its elements, resulting in significant oscillations of the vehicle body. Such conditions increase driver fatigue, slow reaction times, and lead to frequent suspension breakdowns, and wheel separation from the road. These issues, in turn, deteriorate vehicle control and force drivers to reduce speed to mitigate impacts, ultimately lowering the operational efficiency of the vehicle.

Road irregularities on gravel roads often form owing to weak road surfaces, uneven construction, delayed repair of minor defects, low road elevation, and the lack of proper drainable features like slopes and ditches [23].

Certain types of irregularities on granular surfaces are unaffected by soil compaction or the loads applied to the soil. These surfaces are prone to developing lateral ripples (waves), also known as "washboard" or "comb" effects. These patterns form owing to surface forces created by the rolling motion of vehicle wheels. Studies [24] have shown that waves form on earth roads when vehicles travel at speeds over 5.6 km/h. These waves are created as soil particles build up in front of the wheel, eventually forming ridges that grow in height and width over time. Waves on gravel roads tend to form when wheels lock during braking. At high speeds, the wheel often lifts off the ground near the crest of each wave, briefly losing contact with the surface. When the wheel lands after passing the crest, it creates a significant impact, creating additional prerequisites for suspension and new wave formation. There is also a strong influence of the wheel mass and suspension properties on the formation of various wave patterns. Heavy wheels, such as those found in TTMs, create pulsations of higher amplitude and shorter wavelengths.

DOI: https://doi.org/10.17816/0321-4443-628957

STUDY OF MODERN DESIGN SOLUTIONS IN THE FIELD OF INCREASING SMOOTHNESS OF RIDE

Modern vehicle suspensions typically use separate units for damping and elastic elements. However, these elements often fail to provide the smooth ride needed in off-road conditions. When vehicles traverse uneven terrain, vibration acceleration values can become excessively high. This leads to suspension breakdowns and a loss of wheel contact with the road, which reduces the safety of TTM movement.

A key metric for vehicle performance is the average operating speed [1–10], which largely depends on the elastic-damping capabilities of the suspension when operating a TTM in hard-to-reach areas with poor road conditions.

Studies [7] have found that increasing the rigidity of the elastic elements or extending the suspension's dynamic travel can improve the average speed and prevent suspension damage in rough terrains. However, increasing the dynamic travel can be restricted by chassis design constraints and may raise the vehicle's center of mass, which negatively impacts operational safety. Conversely, increasing rigidity can intensify driver discomfort by amplifying vibration disturbances.

At the same time, when TTM is moving over uneven surfaces, the resulting suspension breakdowns indicate insufficient efficiency of their elastic-damping capabilities. Vertical vibration accelerations exceeding 5 m/s^2 force drivers to reduce speed, which can cut the average operating speed of the TTM by 50%. This slowdown results in lower road safety, up to a 70% rise in fuel consumption, a decrease in the overhaul period by up to 40%, and the loss of vibration-sensitive loads (equipment), which damage rates ranging from 15% to 30% [1].

The shortcomings of modern suspensions are tied to their high energy capacity, which arises from the overly rigid characteristics of elastic elements with linear or progressive designs [5, 8, 25]. Such elastic elements struggle to sufficiently absorb vehicle vibrations after crossing uneven surfaces. To reduce the suspension energy capacity, additional elastic elements, such as pneumatic cylinders connected to external energy sources, are sometimes introduced [1–3, 5, 26]. While these additions decrease the energy capacity of the suspension, they transfer more force from road irregularities to suspension travel limiters, ultimately causing a breakdown. Furthermore, these modifications complicate the suspension design and increase costs.

The shock absorber plays a crucial role in ensuring the safe operation of TTMs. Its primary function is to actively dampen vibrations after hitting an obstacle, thereby reducing the rocking motion of the vehicle body [1–10, 12, 13, 26, 27]. Moreover, the elastic elements in the TTM suspension can significantly reduce vibration processes [1–10, 12, 13, 25]. These components must be designed with specific elastic characteristics to effectively minimize the amplitude of oscillations in vehicle's sprung mass when it encounters uneven surfaces. The joint operation of the elastic and damping elements in a TTM's suspension system is essential for achieving optimal ride smoothness. Together, they work to reduce the mean square acceleration of the vehicle body, which reduces driver fatigue, lowers the risk of suspension breakdown, ensures constant contact of the wheel with the road, and leads to better maneuverability of the TTM [4].

The suspension's elastic element plays a critical role not only in ensuring a smooth ride and maintaining constant wheel contact with the road but also in enhancing the lateral stability of TTMs. When operating off-road, irregularities such as slopes or obstacles can cause the vehicle to unload on one side while overloading the other. This imbalance results in body roll, increasing the risk of lateral sliding or overturning, especially when the wheels have insufficient grip on the surface. Changes in the rigidity of the suspension's elastic element directly affect the roll angle of the TTM body [14], since the ability to perceive the load caused by unloading of one side of the vehicle and loading of the other changes. Therefore, efforts to improve ride smoothness must also consider the effect of the suspension's elastic elements and pneumatic tires on the lateral stability of the TTM.

PHSs [1], installed in TTM suspension systems and containing an internal elastic element [22, 28–30], are widely used in off-road conditions. These shock absorbers enable lower energy consumption of the suspension and allow for adjustments to their elastic-damping characteristics. However, they exhibit high stiffness values at the end of the compression stroke. This is caused by the insufficient volume of compressed air and the high pressure in the pneumatic chamber, which ultimately leads to suspension breakdowns. Reducing the high values of the elastic characteristics of such shock absorbers is possible by incorporating an additional pneumatic chamber connected to the internal pneumatic chamber of the absorber. This reduces the relative change in the volume of compressed air at the end of the compression stroke [5].

To further reduce energy consumption and high values of the elastic characteristics of known PHS designs at the end of the compression stroke, a new technical solution is proposed. This design consists of a PHS with an additional pneumatic chamber [31], presented in Fig. 1. It significantly reduces the rigidity and maximum forces in the suspension. As a result, the force impact from irregularities and the natural frequency of body oscillations are reduced.

DOI: https://doi.org/10.17816/0321-4443-628957

PROPOSED TECHNICAL SOLUTION

The developed PHS, presented in Fig. 1 [31], is equipped with an additional pneumatic chamber 5, installed parallel to the main PHS unit. The main PHS features liquid cavities (*B* and *C*) containing shock-absorbing fluid, which are designed to dampen oscillations. It also includes a cylindrical reservoir (cavity *D*) filled with compressed air at a calculated pressure. This reservoir is installed coaxially on the hydraulic part of the shock absorber and, together with the additional pneumatic chamber, absorbs road forces. This design significantly reduces the energy capacity of the PHS's elastic element while providing the required elastic-damping characteristics for effective performance in roadless terrain. In addition, this device allows for the adjustment of gas spring properties, significantly increasing the adaptive capabilities of the suspension. As a result, the proposed technical solution eliminates the need for additional elastic elements in the suspension, thereby simplifying its design.

When the TTM moves, impacts from road irregularities are dampened mainly owing to the elasticity of compressed nitrogen in cavities *D* and *E* when cylinder 3 moves upward relative to cylinder 4 and partially owing to the compression of nitrogen in cavity *A*. During the compression stroke, the volume of cavity *A* decreases as liquid is displaced by rod 15 moving downward relative to cylinder 3. This displacement is compensated by the movement of piston 8.

The damping of oscillation amplitudes after an impact, or attenuation, occurs owing to the hydraulic resistance of piston 7, caused by the liquid flow through the channels and valves of the piston 7.

METHODS OF MATHEMATICAL MODELING OF THE ELASTIC CHARACTERISTIC OF THE PNEUMATIC ELEMENT OF THE PROPOSED TECHNICAL SOLUTION

The characteristics of the PHS pneumatic element are defined by its elastic properties, which can be expressed as a relationship between the vertical load and the elastic element deformation measured directly above the wheel axis [5, 25].

The force exerted by the pneumatic elastic element depends on the initial pressure, the height of the air column, and the effective area of the pneumatic chamber piston. Considering and applying the polytropic law, the equation for the elastic characteristic of the PHS pneumatic element is determined based on the suspension stroke [32]:

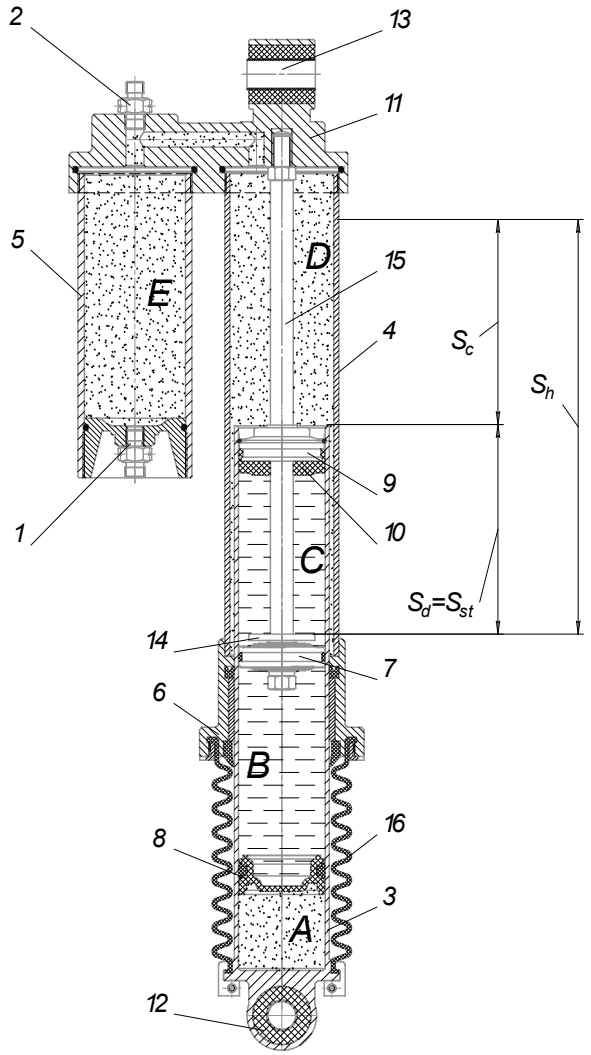

Fig. 1. Design parameters of the pneumohydraulic shock absorber with an additional pneumatic chamber according to the patent for utility model RU № 218675: *A* — a gas compensation cavity; *B* and *C* — lower and upper liquid cavities; *D* and *E* — a gas spring; S_h — total shock absorber stroke; S_d — rebound stroke; S_c and S_{st} — compression stroke and static deformation; *1* — a safety valve; *2* — an adjusting valve; *3* — a lower cylinder; *4* — an upper cylinder; *5* — an additional pneumatic chamber; *6* — a sealing sleeve; *7* — a hydraulic piston; *8* — a pneumatic piston; *9* — a guiding (separating) sleeve; *10* — a damping gasket; *11* — a top cover of the shock absorber; *12, 13* — lugs for shock absorber mounting; *14* — a retaining ring; *15* — a rod; *16* — a protective casing.

Рис. 1. Конструктивные параметры ПГА с дополнительной пневматической камерой по патенту на полезную модель RU № 218675: *A* — газовая компенсационная полость; *B* и *C* — нижняя и верхняя жидкостная полость; *D* и *E* — газовая пружина; S_h — общий ход амортизатора; S_d — ход отбоя; S_c и S_{st} — ход сжатия и статическая деформация; *1* — предохранительный клапан; *2* — регулировочный клапан; *3* — нижний цилиндр; *4* — верхний цилиндр; *5* — дополнительная пневматическая камера; *6* — уплотнительная втулка; *7* — гидравлический поршень; *8* — пневматический поршень; *9* — направляющая (разделительная) втулка; *10* — амортизирующая прокладка; *11* — верхняя крышка амортизатора; *12, 13* — проушины для установки амортизатора; *14* — стопорное кольцо; *15* — шток; *16* — защитный кожух.

$$P = p_{\text{in}} \cdot F_{\text{ef}} \cdot \left(\frac{h_{\text{к}} \cdot i}{h_{\text{к}} \cdot i - \lambda} \right)^n, \quad (1)$$

where p_{in} is the initial pressure, F_{ef} represents the effective area of the pneumatic chamber piston, $h_{\text{к}}$ denotes the height of the air column, i indicates the gear ratio between the wheel stroke and the deformation of the elastic element; λ refers to the wheel stroke, and n is the polytropic index.

The efficiency is analyzed by assessing the reduction in the natural frequencies of the sprung mass of the vehicle obtained from the static position. The natural frequencies of the sprung mass of the vehicle are determined using the equation [1, 2, 9, 10, 20, 21]:

$$w_0 = \sqrt{\frac{c_s}{M}}, \quad (2)$$

where c_s is the stiffness of the elastic element of the shock absorber in the static position, and M is the sprung mass weight that accounts for the wheel.

METHODS OF MATHEMATICAL AND PHYSICAL SIMULATION OF THE OSCILLATORY PROCESS OF VEHICLE MASSES

To study the oscillatory processes of a vehicle, an oscillatory system is used, consisting of several masses connected to each other by elastic-damping bonds [33], allowing for the analysis of the vertical dynamics of oscillations. Specifically, we consider a two-mass oscillatory system (Fig. 2) to evaluate the behavior of the masses in two situations: driving over a single irregularity (unsteady oscillations, Fig. 2*a*) and facing the most unfavorable conditions, such as driving over sinusoidal irregularities (Fig. 2*b*), i.e., under steady (forced) oscillations.

When investigating unsteady oscillations, any irregularities in the adjacent sections of the road are neglected, assuming that prior to encountering the irregularity, the system was stationary, meaning that the vehicle was not oscillating. A single irregularity is used for this analysis because the oscillations largely depend on the specific road section where the oscillating system is located at that moment. Therefore, we consider the largest irregularity, while the effect of smaller irregularities is assumed to be minimal [10]. This analysis allows us to analyze the motion of the system as it transitions from rest to free oscillations, after the transient phase. These free oscillations help ascertain the degree of damping and the stability of the wheel contact with the road.

For steady (forced) oscillations, which result from sinusoidal irregularities, the transition process from unsteady oscillations to steady oscillations is considered [10]. Although steady oscillations occur less frequently, they represent one of the most demanding operating conditions for the suspension. This scenario is critical as it can lead to short-term loss of wheel contact between with the road. This type of oscillation also enables to closely simulate the TMM movement along the comb.

The mathematical model of the oscillation systems under consideration is described using the following system of two second-order differential levels [20,33–36]:

$$\begin{cases} m \cdot \ddot{z}_1 + r_t\left(\dot{z}_1 - dn\right) + r\left(\dot{z}_1 - \dot{z}_2\right) + c_t\left(z_1 - n\right) + c_s\left(z_1 - z_2\right) = 0, \\ M \cdot \ddot{z}_2 + r\left(\dot{z}_2 - \dot{z}_1\right) + c_s\left(z_2 - z_1\right) = 0, \end{cases} \quad (3)$$

where dn and n are the disturbance functions from the road (displacement and speed).

Road disturbance functions for a single irregularity calculated using the following equations [20,33–36]:

$$dn = \frac{\pi VaH}{l} \sin\left(2\pi \frac{s - S0}{l}\right)\left(\Phi\left(s - S0\right) - \Phi\left(s - S0 - l\right)\right), \quad (4)$$

$$n = \frac{H}{2}\left(1 - \cos\left(2\pi \frac{s - S0}{l}\right)\right)\left(\Phi\left(s - S0\right) - \Phi\left(s - S0 - l\right)\right), \quad (5)$$

where Φ is the Heaviside function.

Road disturbance functions for a sinusoidal irregularity were calculated using the following equations [20,33–36]:

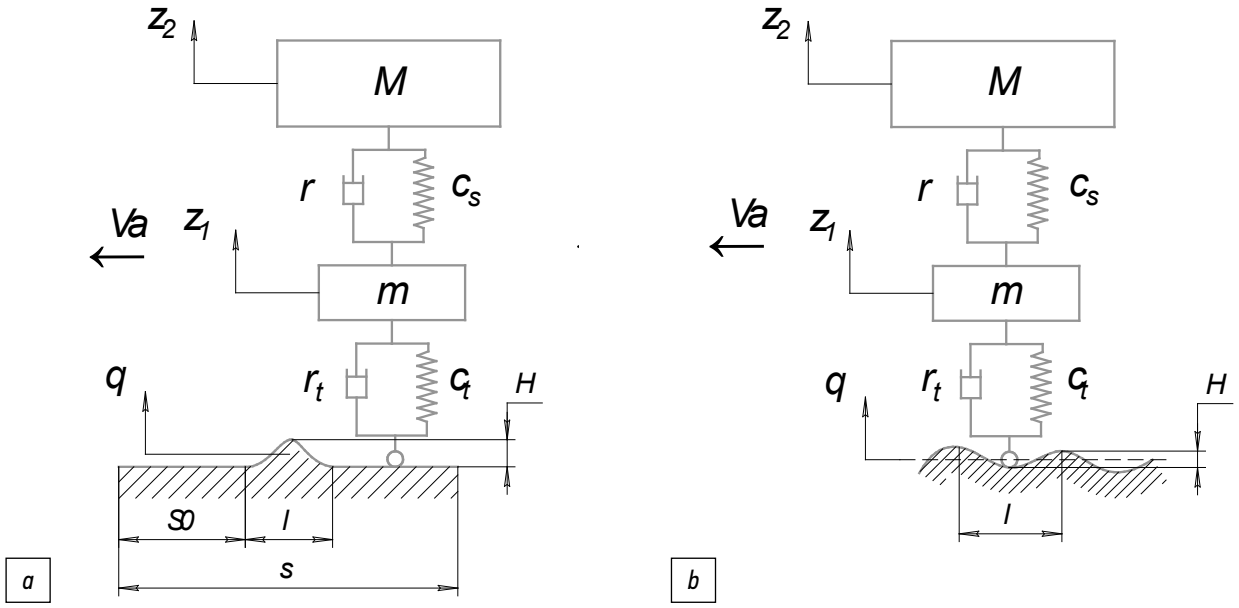

Fig. 2. Calculation scheme of a two-mass oscillating system: *a* — passing a bump; *b* — passing a sinusoidal bump; *M* — sprung mass; *m* — unsprung mass; c_s — gas spring stiffness of the shock absorber; c_t — tire stiffness; *r* — damping capacity of the shock absorber; r_t — damping capacity of the tires; z_1, z_2 — vertical displacement of unsprung and sprung mass; *Va* — direction of motion (velocity); *q* — kinematic disturbance; *S0* — beginning of a bump; *s* — considered section of the road; *l* — length of a bump; *H* — height of bumps.
Рис. 2. Расчетная схема двухмассовой колебательной системы: *a* — проезд неровности; *b* — движение по синусоидальной неровности; *M* — подрессоренная масса; *m* — неподрессоренная масса; c_s — жесткость газовой пружины амортизатора; c_t — жесткость шин; *r* — демпфирующая способность амортизатора; r_t — демпфирующая способность шин; z_1, z_2 — вертикальное перемещение неподрессоренной и подрессоренной массы; *Va* — направление движения (скорость); *q* — кинематическое возмущение; *S0* — начало неровности; *s* — рассматриваемый участок пути; *l* — длина неровности; *H* — высота неровностей.

$$dn = H \cdot \omega_q \cdot \cos\left(\omega_q \cdot t\right), \quad (6)$$

$$n = H \cdot \sin\left(\omega_q \cdot t + \varphi\right), \quad (7)$$

where ω_q is the specified frequency of the external disturbance, φ represents the phase shift, and t denotes the considered time interval of the oscillatory process.

To solve the given differential equation system (3), the Mathcad software environment employs the Runge–Kutta method with an adapted integration step. The stability and accuracy of the numerical solution depend on the size of the integration step. The smaller the step, the higher the calculation accuracy. This step is determined by the number of calculation points. Increasing the number of points reduces the step size. Furthermore, to obtain numerical results for calculating Eq. (3), the Mathcad package has a special function Rkadapt that checks how quickly the approximate solution changes and adapts the step size, allowing to increase calculation accuracy [20,33–36]. Before solving, the system of equations (3) is transformed into the Cauchy form, where generalized system variables (mathematical variables) are replaced by machine variables corresponding to Mathcad's variables.

The resulting displacements of the vehicle masses as it moves over road irregularities are analyzed by calculating the acceleration values of these masses, while their spread reaches large values. The system of differential equations (3), reduced to the Cauchy form, does not allow for a direct numerical solution of mass acceleration. Therefore, for the numerical solution of mass acceleration, the following equation was used [9, 10, 20, 21]:

$$a = w_0^2 \cdot z, \quad (8)$$

where z is the vertical mass displacement.

METHODS FOR ASSESSING THE INFLUENCE OF THE STIFFNESS OF THE ELASTIC SUSPENSION ELEMENT AND PNEUMATIC TIRES ON THE STATIC LATERAL STABILITY OF THE VEHICLE

To assess the effect of increasing the ride smoothness on the TTM lateral stability, a turnover scheme (Fig. 3) was considered. This scheme highlights the most heavily loaded rear axle of the KAMAZ 43502 truck. When

modeling the TTM stability, the angular deviation of the body mass was considered. This included the angular deformation of the suspension's elastic elements where one side unloads and the other side bears additional load. It accounted for the proposed PHS and the pneumatic tires, both of which deform during a roll. Furthermore, factors such as the height of the center of gravity, the difference in wheel track width, and the installation of the PHS were considered.

The main parameter for assessing lateral stability on a slope, according to GOST 31507-2012, is the lateral stability coefficient of the vehicle [12–19, 37, 38]. This coefficient helps determine the angle of static stability for lateral overturning and the permissible angle of body roll. According to GOST 31507-2012, the angle of body roll ranges from 6.5° to 8.4°, while the minimum permissible value for the static stability angle is 21° across all vehicle trajectories [12, 38].

The lateral stability coefficient is determined by the equation [38]:

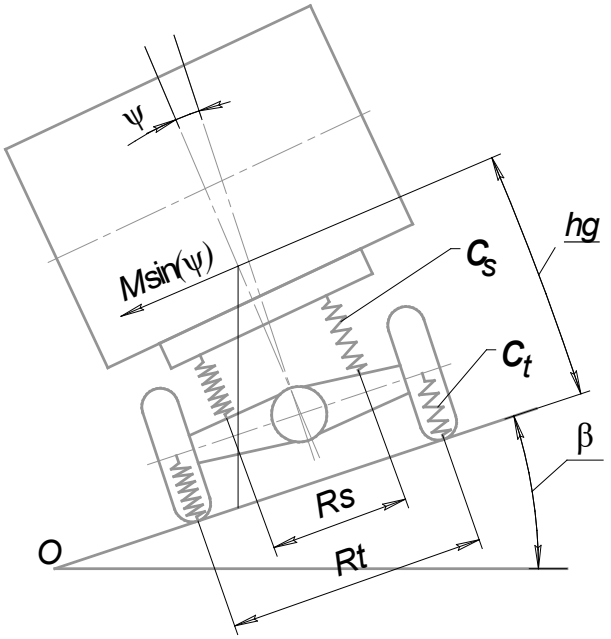

Fig. 3. Calculation scheme of the machine under static transverse stability: Rt — average tire track, m; Rs — mounting distance of shock absorbers in the suspension, m; hg — height of the center of mass, m; c_s — stiffness of the elastic element of the shock absorber, N/m; c_t — stiffness of pneumatic tires, N/m; $M\sin(\psi)$ — transverse component of the gravity force; ψ — body roll angle; β — angle of the transverse slope of the road.

Рис. 3. Расчётная схема подрессоривания машины при статической поперечной устойчивости: Rt — средняя колея шин; Rs — расстояние установки амортизаторов в подвеске; hg — высота центра масс; c_s — жёсткость упругого элемента амортизатора; c_t — жёсткость пневматических шин; $M\sin(\psi)$ — поперечная составляющая силы тяжести; ψ — угол крена кузова; β — угол поперечного наклона дороги.

$$\eta = \frac{Rt}{2 \cdot hg}. \quad (9)$$

The standard value of the static stability angle for lateral overturning according to GOST 31507-2012, depending on the lateral stability coefficient, is determined using the following equations [12, 37, 38]:

$$\begin{cases} \beta_{kt} = 42,4 \cdot \eta - 2,4; \quad \text{with} \quad 0,55 \le \eta \le 1,0, \\ \beta_{kt} = 25 \cdot \eta + 15; \quad \text{with} \quad \eta > 1,0. \end{cases} \quad (10)$$

However, these equations do not consider the influence of the suspension's elastic elements and pneumatic tire characteristics on lateral stability. To address this, the lateral stability coefficient was derived by including the angular deformation of the proposed PHS elastic elements and the pneumatic tires occurring during roll. The coefficient was calculated using the following equation [14, 37]:

$$\eta = \frac{Rt}{2 \cdot hg} - \frac{Ga}{2 \cdot c_t \cdot Rt} - \frac{Ga}{c_s \cdot Rs}, \quad (11)$$

where Ga is the overturning force.

The transverse component $M\sin(\psi)$ of the vehicle gravity, having an arm hg, forms an overturning force that accounts for the elastic properties of the elastic elements of the suspension and pneumatic tires [14, 37]:

$$Ga = \frac{2 \cdot c_s \cdot Rs \cdot \sin(\psi)}{2 \cdot Rs} + \frac{2 \cdot c_t \cdot Rt \cdot \sin(\psi)}{Rt}. \quad (12)$$

The angle of static stability for lateral overturning at the moment one wheel lifts off the road is determined by the following equation:

$$\beta_{kt} = \text{arctg}(\eta). \quad (13)$$

The loss of vehicle stability involves overturning, which leads to far more serious consequences compared to sliding. Therefore, it is necessary to ensure that the vehicle parameters and suspension properties are designed to prevent overturning. Stability must begin to fail with lateral sliding on a slope. In order for lateral sliding to precede lateral overturning, the following condition must be met [12–19, 37]:

$$\eta > \varphi, \quad (14)$$

where φ is the coefficient of tire adhesion to the road.

The slope angle for the lateral slip is determined using the following equation [12–19, 37]:

$$\beta_{ks} = \text{arctg}(\varphi). \quad (15)$$

RESULTS OF A PRACTICAL STUDY OF THE ELASTIC CHARACTERISTIC OF THE PNEUMATIC ELEMENT OF THE PROPOSED TECHNICAL SOLUTION

To assess the efficiency of using an additional pneumatic chamber and its effect on the natural frequencies of body oscillations, we compare the elastic characteristics of a design with and without the additional pneumatic chamber. Since the TTM under consideration has repair equipment on board, the vehicle's mass change is negligible.

The data used to construct the elastic characteristic were obtained during the vehicle design process (Table 1).

The results of the mathematical analysis of the PHS elastic characteristics are presented in Fig. 4. These results indicate that the elastic characteristic with the additional pneumatic chamber (line 2, Fig. 4) exhibits a flatter curve compared to the design without it (line 1, Fig. 4), which leads to a significant decrease in the elastic element rigidity at the end of the suspension travel.

The intersection of the lines at the static load point occurs because the initial parameters for the pneumatic shock absorber system were based on the calculated force under static load P_{st} of the equipped vehicle. It is used to calculate the forces of dynamic compression S_c and rebound S_{ds}. The position of the static load depends on the specified initial gas pressure and its volume in the chambers. Therefore, the parameters of the elastic characteristic may vary.

RESULTS OF A PRACTICAL STUDY OF OSCILLATORY PROCESSES OF VEHICLE MASSES

Reducing suspension rigidity by connecting an additional gas chamber significantly reduces both the rigidity and maximum forces in the suspension, which in turn decreases the force impact and the natural frequency of body oscillations. Consequently, the relative damping coefficient for both the body and the wheels increases, leading to improved overall vehicle oscillation dynamics. For this purpose, a linear two-mass mathematical model of a single-support suspension was developed based on Eq. (3). This model replaces the nonlinear characteristics of the PHS with linear approximations (Fig. 4 and Table 2). Suspension compression breakdown and wheel-road separation during rebound were excluded from the analysis since these events are unlikely to occur. The model was evaluated using Mathcad software, applying the Runge–Kutta numerical method with an adapted integration step.

For transient oscillation analysis caused by a single irregularity, zero initial conditions were set. This allowed the irregularity of the adjacent road sections to be ignored. Similarly, for the study of steady-state oscillations owing to sinusoidal irregularities, zero initial conditions were used. However, these sinusoidal irregularities were assumed to maintain a steady-state form over the entire road section under consideration. The kinematic disturbance of oscillations for both scenarios was defined using specific functions and their derivatives, described by Eqs. (4)–(7).

A graphical interpretation of the numerical results for driving over a single 0.08 m high and 3 m long irregularity at 30 km/h is presented in Fig. 5.

Table 1. Initial data for construction of elastic characteristics of suspension on the basis of KAMAZ 43502 truck chassis in loaded condition
Таблица 1. Исходные данные для построения упругой характеристики подвески на базе шасси грузового автомобиля КАМАЗ 43502 в снаряженном состоянии

Parameter	Value
Sprung mass accruing to the rear wheel, kg	3071,00
Unsprung mass accruing to the rear wheel, kg	629,00
Static load accruing to the rear wheel, kN	30,10
Static suspension travel, m	0,14
Dynamic suspension deflection, m	0,14
Suspension travel at which the compression buffer is triggered, m	0,21
Suspension travel at which the rebound bumper is triggered, m	0,03
Full suspension travel, m	0,28
Rigidity of the KAMA-URAL 390/95R20 pneumatic tire, N/m	$8{,}19 \cdot 10^5$
Resistance coefficient of the KAMA-URAL 390/95R20 tire, N·s/m	$6{,}60 \cdot 10^{-4}$
Suspension gear ratio	1,10

DOI: https://doi.org/10.17816/0321-4443-628957

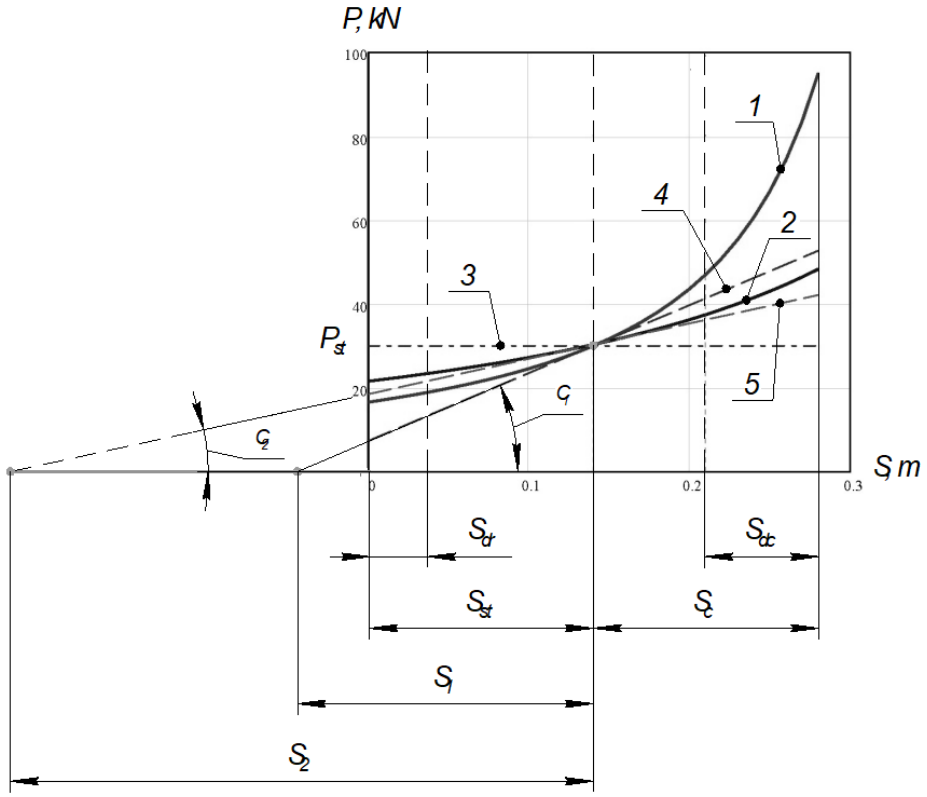

Fig. 4. Results of modeling the elastic characteristic of the PGA: *1* — gas spring force without additional chamber; *2* — gas spring force with additional chamber; *3* — line showing the shock absorber position under static load; *4* — tangent line to the static load occurring in the design without additional chamber; *5* — tangent line to the static load occurring in the structure with additional chamber; S_{dr} — rebound stroke; S_c — compression stroke; S_{dc} — suspension stroke at which the rebound buffer is activated; S_{st} — static stroke; C_1 — angle of inclination to the tangent line 4; C_2 — angle of inclination to the tangent line 5; S_1 and S_2 — reduced static deflections.
Рис. 4. Результаты моделирования упругой характеристики ПГА: *1* — сила газовой пружины без дополнительной камеры; *2* — сила газовой пружины с дополнительной камерой; *3* — линия, показывающая положение амортизатора под статической нагрузкой; *4* — касательная линия к статической нагрузке, возникающая в конструкции без дополнительной камеры; *5* — касательная линия к статической нагрузке, возникающая в конструкции с дополнительной камерой; S_{dr} — ход отбоя; S_c — ход сжатия; S_{dc} — ход подвески, при котором срабатывает буфер отбоя; S_{st} — статический ход; C_1 — угол наклона к касательной линии 4; C_2 — угол наклона к касательной линии 5; S_1 и S_2 — приведенные статические прогибы.

Table 2. Suspension parameters with installed PGA of KAMAZ 43502 truck
Таблица 2. Параметры подвески с установленными ПГА грузового автомобиля КАМАЗ 43502

Parameter	Value	
	PHS with additional chamber	PHS without additional chamber
Rigidity of the elastic element of the shock absorber under static load, kN/m	73,70	150,30
Rigidity of the elastic element of the shock absorber at the final stroke of the suspension, kN/m	177,60	1581,00
Drag coefficient of the shock absorber, N·s/m	8403,00	12520,00
Frequency of partial low-frequency oscillations of the body, Hz	0,78	1,11
Circular frequency of natural oscillations of the unsprung mass, Hz	6,00	6,25
Damping coefficient of oscillations of the sprung mass, rad/s	1,37	2,04
Aperiodicity coefficient of the rear sprung mass	0,28	0,29
Relative damping coefficient of unsprung mass oscillations	0,18	0,29
Coefficient of absorption capacity of the elastic element of the shock absorber	1,60	3,16

The curves of the vehicle's damped oscillations reveal that the greatest displacements occur as the vehicle passes over the irregularity. Once the wheel leaves the irregularity, the oscillations gradually subside. The movement of the sprung mass (line *Z*2, Fig. 5*a* and *c*) shows a phase shift relative to the unsprung masses (line *Z*1, Fig. 5*a* and *c*). This shift occurs because, upon driving over an irregularity, the unsprung mass responds first, followed by the body. Using the proposed PHS, the movement of the unsprung masses when encountering the irregularity does not exceed its specified height, demonstrating that the wheel closely follows the road's irregularity profile.

When using a PHS without an additional pneumatic chamber (Fig. 5*c*), the body exhibits significant movement upon encountering an irregularity, often exceeding the height of the irregularity itself. After passing the irregularity, prolonged oscillatory processes of the masses are registered. Furthermore, body acceleration reaches high levels (Fig. 5*d*), increasing driver fatigue and compelling the driver to reduce the TTM speed to reduce discomfort caused by the road irregularities.

Conversely, when using a PHS with an additional pneumatic chamber (Fig. 5*a*), the body movement upon hitting an irregularity remains below the irregularity height and is reduced by 15.8% compared to the design without a pneumatic chamber. Suspension breakdown does not occur as the movement of the unsprung mass stays within the maximum dynamic deformation limit of the suspension, set at 0.14 m during simulations. After the wheel passes the irregularity, free vibrations fade within four seconds. Body acceleration, presented in Fig. 4*b*, is significantly decreased by 2.6 times, highlighting the effective absorption capacity of the proposed PHS. As a result, the driver does not have

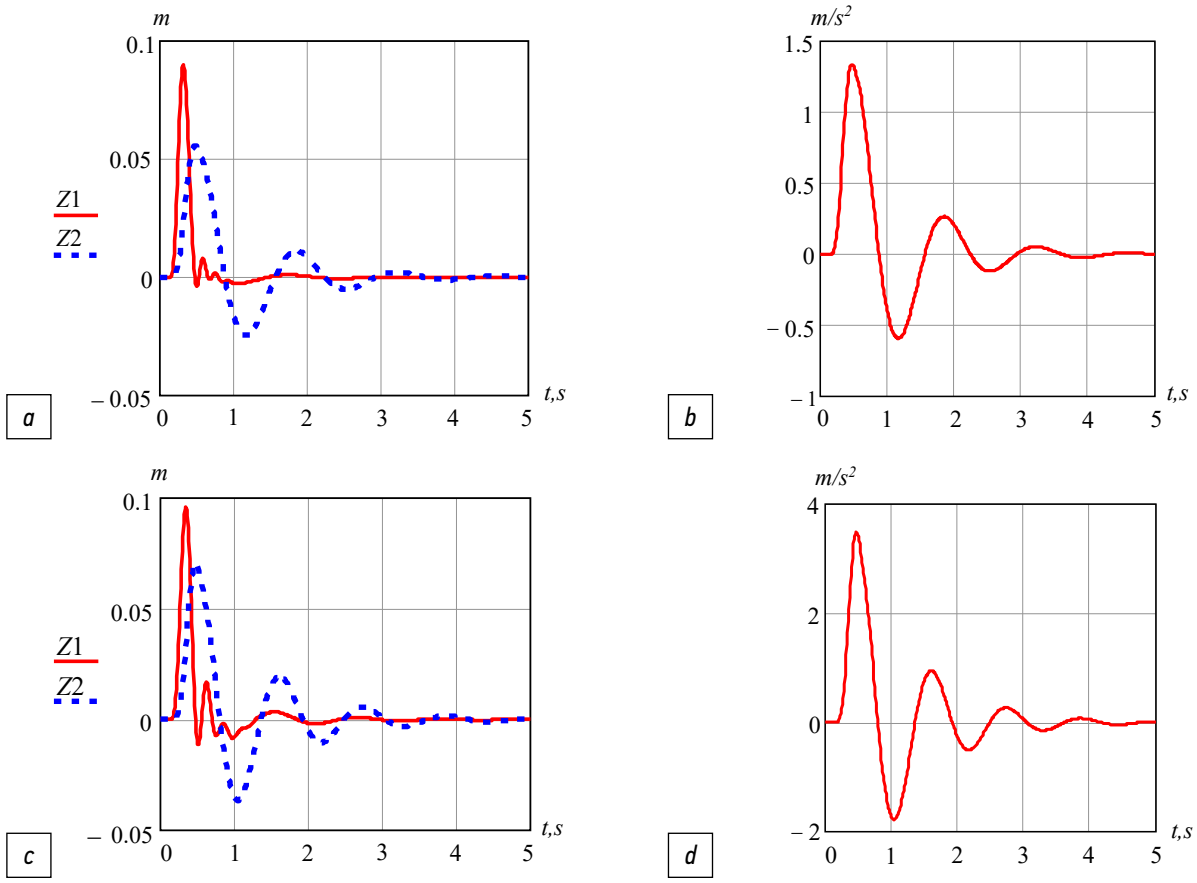

Fig. 5. Unsteady oscillatory process of the mass of the machine in time *t* (sec.), resulting from the passage of a single bump: Z1 and Z2 — displacement of unsprung and sprung masses; *a* — displacement (stroke) of the machine masses without the additional chamber; *b* — acceleration of the body without the additional chamber; *c* — displacement (stroke) of the car masses with the additional chamber; *d* — acceleration of the body with the additional chamber.

Рис. 5. Неустановившийся колебательный процесс масс машины по времени *t* (сек.), полученный в результате проезда единичной неровности: Z1 и Z2 — перемещение неподрессоренной и подрессоренной массы; *a* — перемещение (ход) масс машины с установленным в подвеску амортизатора, имеющий дополнительную пневмокамеру; *b* — ускорение подрессоренной массы в случае использовании амортизатора с дополнительной пневмокамерой; *c* — перемещение (ход) масс машины с установленным в подвеску амортизатора, не имеющего дополнительную пневмокамеру; *d* — ускорение подрессоренной массы в случае использовании амортизатора без дополнительной пневмокамеры.

DOI: https://doi.org/10.17816/0321-4443-628957

to slow down, since this irregularity no longer causes discomfort. According to studies [1], typical peak vibration accelerations in trucks range from 4 to 5 m/s^2. In However, with the proposed PHS, the maximum body acceleration is limited to 1.35 m/s^2, demonstrating its effectiveness.

A graphical interpretation of the steady-state oscillation calculations for driving over a sinusoidal irregularity, which represents the most demanding suspension operation mode (movement over a comb-like pattern), is presented in Fig. 6. The height of this irregularity is 0.08 m, and its length is 3 m with a disturbance frequency ω_q of 17. 45 s^{-1}, which corresponds to a TTM speed of 30 km/h.

The analysis of the obtained steady-state oscillations of the vehicle masses shows that, with the proposed PHS, wheel displacement does not exceed the height of the irregularity. Similarly to passing over a single irregularity, a phase shift is observed between the vehicle masses. After an initial transient phase lasting approximately 1 s, the oscillations transition to a steady state The displacements of the vehicle masses and their accelerations reach high values when hitting the irregularity.

Using the PHS with an additional pneumatic chamber (Fig. 6*c* and *d*) results in more steady-state oscillations of the vehicle masses after the transient process, while ensuring constant contact of the wheel with the road. This allows the wheels to follow the irregularity closely, reducing the body displacements by 25%, and, consequently, its accelerations by 2.6 times. During the transient process, peak body acceleration reaches just 0.8 m/s^2, significantly lower than the typical vibration acceleration in trucks, which ranges from 4 to 5 m/s^2 [1]. After the transient process, body acceleration stabilizes at 0.4 m/s^2, enabling the vehicle to drive on this irregularity

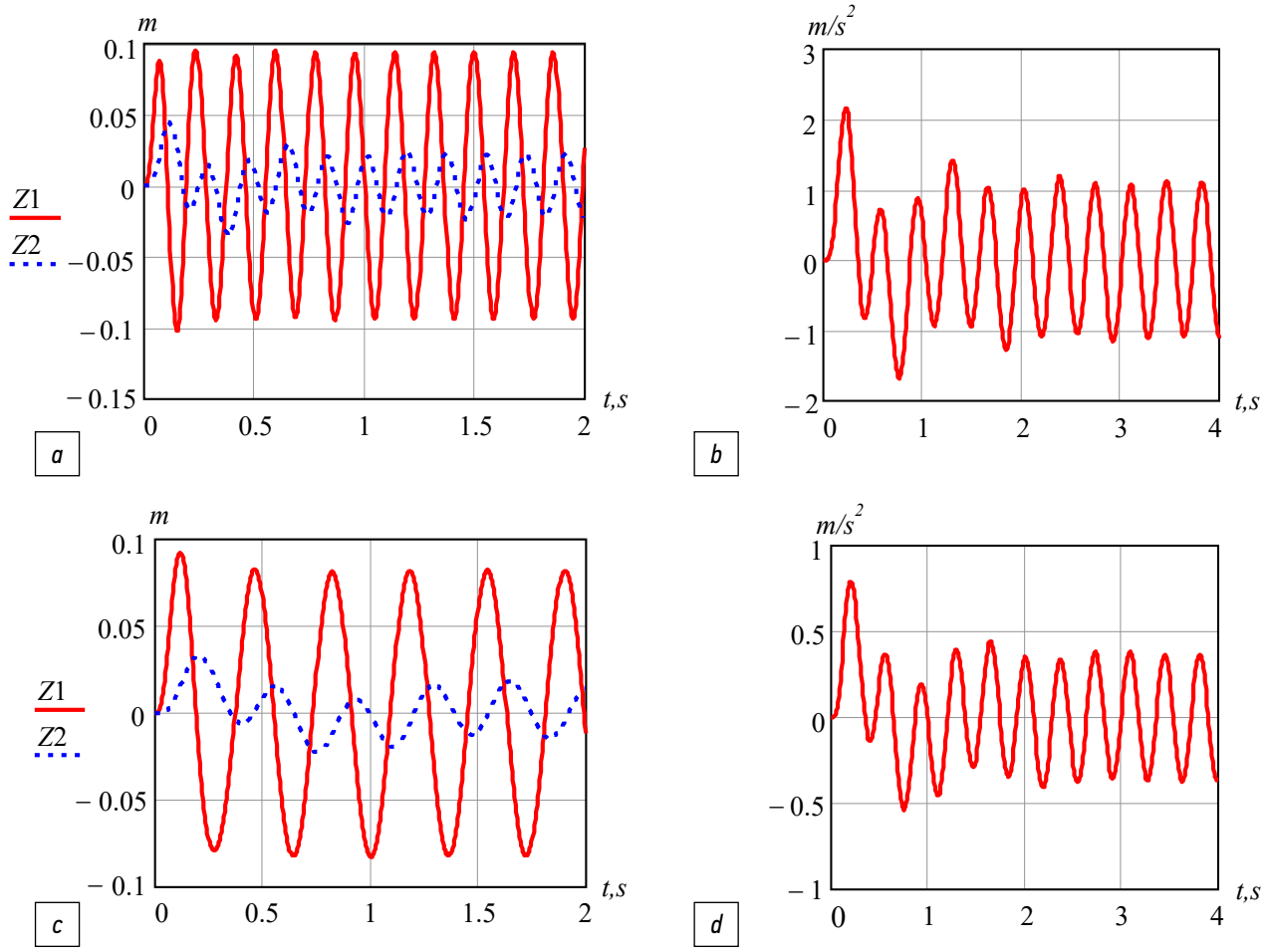

Fig. 6. Characteristics of steady-state oscillatory processes of the car masses by time *t* (sec.), obtained as a result of passing a sinusoidal bump: Z1 and Z2 — displacement of unsprung and sprung masses; *a* — displacement (stroke) of the car masses without an additional chamber; *b* — acceleration of the body without an additional chamber; *c* — displacement (stroke) of the car masses taking into account an additional chamber; *d* — acceleration of the body taking into account an additional chamber.

Рис. 6. Характеристика установившихся колебательных процессов масс машины по времени *t* (сек.), полученные в результате проезда синусоидальной неровности: Z1 и Z2 — перемещение неподрессоренной и подрессоренной массы; *a* — перемещение (ход) масс автомобиля без дополнительной камеры; *b* — ускорение кузова без дополнительной камеры; *c* — перемещение (ход) масс автомобиля с учетом дополнительной камеры; *d* — ускорение кузова с учетом дополнительной камеры.

DOI: https://doi.org/10.17816/0321-4443-628957

for 480 minutes without causing excessive driver fatigue. This complies with the regulatory limits for vertical accelerations over specific exposure times as presented in GOST 31191.1-2004 [1–3, 39, 40]. When driving a vehicle equipped with the proposed PHS at a resonant speed of 8.6 km/h over a single irregularity, the movements of the sprung masses increase to 0.11 m, causing their accelerations to reach 2.6 m/s^2. Over sinusoidal irregularities, peak acceleration values of the sprung masses rise to 3.2 m/s^2. These values enable the vehicle to handle such irregularities for 60 minutes. However, driving in resonant mode can lead to increased loads on the vehicle units and components, as well as increased discomfort for the driver and passengers.

The simulation analysis shows that the amplitude of the oscillations depends on the disturbance frequency, which is influenced by the TTM speed and the length of the irregularity.

RESULTS OF A PRACTICAL STUDY OF STATIC TRANSVERSE STABILITY OF A VEHICLE ON A SLOPE

A decrease in the rigidity of the suspension's elastic element can negatively compromise vehicle stability when moving on a slope. To analyze how an additional pneumatic chamber affects stability, we use the calculation scheme presented in Fig. 3. The initial data include the rigidity values for the PHS and pneumatic tires, as detailed in Tables 2 and 3. The most dangerous is modeled, where the roll angle of the body reaches its maximum, causing unloading on one side and load the other side.

Table 3. Initial data for determination of machine stability on slope
Таблица 3. Исходные данные для определения устойчивости машины на косогоре

Parameter	Value
Distance between elastic elements of suspension (PHS), m	0,57
Average track of tires, m	1,92
Height of the center of mass, m	0,98
Body roll angle, deg	8,40

Using a single-mass model to simulate this worst-case scenario, with a body roll angle of 8.4°, the lateral stability coefficient was calculated at 0.932, and the critical slope angle for lateral rollover was 43°. Values calculated according to the methodology proposed in GOST 31507-2012, yielded a lateral stability of 0.98 and a critical slope angle of 38°, with a calculated body roll angle of 6.5°. These results demonstrate that as the roll angle approaches critical values, the lateral stability coefficient decreases. However, the road's lateral slope angle exceeds the static stability angle for lateral rollover, obtained without considering the elastic properties of the PHS and pneumatic tires. This demonstrates the importance of including suspension and tire characteristics when evaluating vehicle static stability.

The relationship between suspension rigidity and static stability angle, as modeled in Mathcad [37] using the proposed technical solution (Fig. 7), indicates that reducing the rigidity of the PHS elastic element does not cause a significant decrease in the angle of static stability and even exceeds the standard values. If a regulating pneumatic valve is installed between the primary and additional pneumatic chambers of the PHS, particularly on the side facing the slope, the static stability angle can be increased to 44°. According to the presented graph (Fig. 7), rigidity values ranging from 50 kN/m to 1,000 kN/m affect the angle of static stability on the slope. Beyond this range, increased rigidity no longer improves TTM stability.

The study assumes static conditions. Under dynamic conditions, with oscillations of the sprung masses on the elastic elements of the suspension, the stability angle can decrease. However, owing to the reduced oscillations with the proposed PHS, the dynamic stability remains nearly unchanged.

Table 4 presents the calculated lateral slip angles for different road surface types and conditions commonly found in roadless terrain. These values were obtained for the KAMA-URAL 390/95R20 [41] high-traffic tires, which are installed on the chassis of the KAMAZ 43502 truck.

The results (Table 1), reveal that the maximum lateral slip angle is 35°, significantly lower than the calculated static stability angle for lateral turnover, which is 43°. This ensures the vehicle slides smoothly down the slope rather than overturning, thereby satisfying the condition of Eq. (14), and enhancing the safety of TTM operation in roadless terrain.

CONCLUSION

The safety of TTM operation in off-road conditions depends on various vehicle parameters and their interaction in the oscillatory system. The presented calculation methods for oscillatory systems allow for analyzing these processes, assessing the effect of the additional pneumatic chamber in the PHS, and evaluating its effect on key indicators of traffic safety in off-road conditions.

The study found that when encountering a single irregularity, the proposed PHS reduced body movement

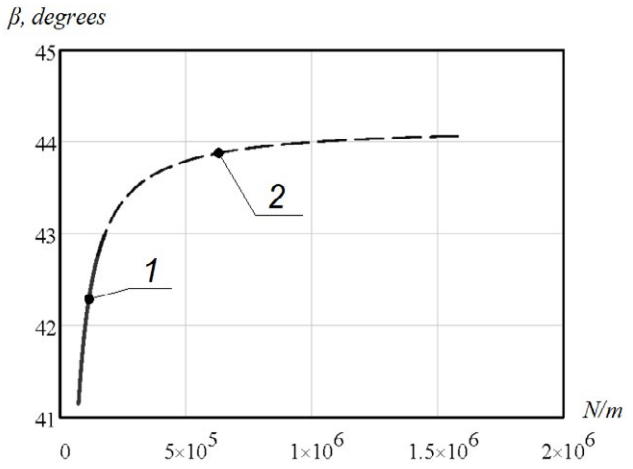

Fig. 7. Influence of the stiffness of the elastic element of the shock absorber on the static transverse stability of the machine on a slope: *1* — dependence when using a PHA with an additional pneumatic chamber; *2* — dependence when using a PHA without an additional pneumatic chamber.

Рис. 7. Влияние жёсткости упругого элемента амортизатора на статическую поперечную устойчивость машины на косогоре: *1* — зависимость при использовании ПГА с дополнительной пневматической камерой; *2* — зависимость при использовании ПГА без дополнительной пневматической камеры.

by 15.8% at the point of impact and decreased body acceleration by 2.6 times. Furthermore, the oscillatory motions of the vehicle masses completely dampened in period 4. The wheel follows the profile of the irregularity without causing a breakdown of the suspension.

For the most demanding conditions, such as driving on a comb-shaped sinusoidal irregularity, the proposed PHS stabilized the oscillatory movements of the vehicle masses significantly. The wheels adapted to the wave irregularity without damaging the suspension, decreasing body movements by 25%. Body acceleration during the stabilized oscillatory process also reduced by 2.6 times. Consequently, the TTM could traverse such uneven surfaces at a speed of 30 km/h for 480 min without increasing driver fatigue.

The study also determined that critical parameters such as TTM speed along uneven surfaces, the frequency of impacts from these surfaces, and their lengths affect significantly the oscillatory system.

The presented method for assessing the static stability of a vehicle on a slope can be used to assess vehicle stability, considering the elastic characteristics of the suspension elements and pneumatic tires. The study showed that with a maximum permissible body roll angle of 8.4°, the angle of static stability for lateral rollover reached 43°. This value is 13.2% higher than results calculated using the method presented in GOST 31507-2012.

The PHS elastic element rigidity was found to significantly influence the angle of static stability for lateral overturning in the range of 50–1,000 kN/m. Beyond this range, further increases in rigidity have minimal effect on stability but negatively affect ride smoothness. At the same time, dynamic stability remains largely unaffected by these changes.

ADDITIONAL INFORMATION

Author's contribution. R.R. Bukirov — development of a technical solution in the form of a pneumohydraulic shock absorber with an additional pneumatic chamber, development of a methodology for mathematical modeling of two-mass single-axis oscillating systems under steady and unsteady oscillations, development of a mathematical apparatus for estimating the transverse stability of the machine taking into account the elastic response of the suspension element and the most pneumatic tires, search for publications on the topic of the article, writing the manuscript text, editing the manuscript text, creating images. The author confirms the compliance of his authorship with the ICMJE international criteria (the author has made a significant contribution to the conceptualization, research and preparation

Table 4. Side slip angles for different types of road surfaces and their state

Таблица 4. Углы по боковому скольжению при различных типах поверхностях дорог и их состояния

Surface type and its condition	Lateral slip angle, degrees
Dry cobblestone	35,0
Crushed stone:	
dry	35,0
wet	28,8
Soil:	
dry	31,0
wet	26,6
waterlogged	16,7
Sandy:	
dry	16,7
wet	26,6
Loamy:	
dry	26,6
wet	24,2
waterlogged	14,0
Snowy:	
loose	21,8
compacted	26,6
Icy	5,7

of the article, read and approved the final version before publication).

Competing interests. The author declares that they have no competing interests.

Funding source. The author declares that there was no external funding when conducting the research and preparing the publication.

Acknowledgments. The author expresses gratitude to the reviewer for valuable comments and remarks that contributed to the improvement of this article for its publication in the journal.

ДОПОЛНИТЕЛЬНАЯ ИНФОРМАЦИЯ

Вклад автора. Р.Р. Букиров — разработка технического решения в виде пневмогидравлического амортизатора с дополнительной пневматической камерой, разработка методики математического моделирования двухмассовых одноопорных колебательных систем при установившихся и неустановившихся колебаниях, разработка математического аппарата для оценки поперечной устойчивости машины с учётом упругой характеристики элемента подвески и самых пневмошин, поиск публикаций по теме статьи, написание текста рукописи, редактирование текста рукописи, создание изображений. Автор подтверждает соответствие своего авторства международным критериям *ICMJE* (автор внес существенный вклад в разработку концепции, проведение исследования и подготовку статьи, прочёл и одобрил финальную версию перед публикацией).

Источник финансирования. Автор заявляет об отсутствии внешнего финансирования при проведении исследования и подготовке публикации.

Конфликт интересов. Автор декларирует отсутствие явных и потенциальных конфликтов интересов, связанных с проведенным исследованием и публикацией настоящей статьи.

Благодарности. Автор выражает благодарность рецензенту, за ценные комментарии и замечания, способствовавшие улучшению данной статьи для её публикации в журнале.

REFERENCES

1. Novikov VV, Ryabov IM, Chernyshov K.V. *Vibration-protective properties of suspensions of motor vehicles.* Moscow, Vologda: Infra-Inzheneriya; 2021. (In Russ.) EDN: FRSPKX

2. Novikov VV, Chernyshov KV, Pozdeev AV, et al. *Combined damping systems in suspensions of motor vehicles.* Moscow; Vologda: Infra-Inzheneriya; 2024. (In Russ.)

3. Novikov VV, Chernyshov KV, Pozdeev AV. *Calculation of the systems of motor vehicles suspension.* Moscow; Vologda: Infra-Engineering; 2024. (In Russ.)

4. Repin SV, Bukirov RR, Vasilieva PV. Study on effects of damping characteristics of base chassis suspension on operational safety of transport and handling machinery. In: *Transportation Research Procedia: 14, Saint Petersburg, October 21–24, 2020.* Saint Petersburg; 2020:574–581. doi: 10.1016/j.trpro.2020.10.069 EDN: MTWSYH

5. Repin S, Bukirov R, Vorontsov I, et al. Improving the movement smoothness of a mobile repair shop for machinery servicing in the Arctic // *Transportation Research Procedia, St. Petersburg, 02–04 June 2021.* St. Petersburg, 2021;553–561. doi: 10.1016/j.trpro.2021.09.084 EDN: DJBMGB

6. Bukirov RR. Modeling of damping processes of suspension damping of transport-technological means on the basis of automobile chassis in the Arctic operating conditions. In: *Technical provision of accessibility of the Arctic regions: Proceedings of the III All-Russian scientific seminar, St. Petersburg, October 27, 2022.* St. Petersburg State University of Architecture and Civil Engineering, 2022:57–65. (In Russ.) EDN: EAMVYY

7. Dubrovskiy AF, Abramov MI, Sakulin YuA. Selection of suspension parameters of "Ural" trucks to increase the speed of movement on worn-out dirt roads. *Bulletin of Orenburg State University.* 2014;10(171):66–75 (In Russ.) EDN: TPNREB

8. Repin SV, Maslennikov NA, Orlov DS, et al. Investigation of the processes of smooth running of transport-technological machines based on truck chassis in difficult road conditions. *Transport, Mining and Construction Engineering: Science and Production.* 2023;23:76–84. (In Russ.) doi: 10.26160/2658-3305-2023-23-76-84 EDN: UMNUWF

9. Reimpel Y. *Car chassis: Shock absorbers, tires and wheels.* Moscow: Mashinostroenie; 1986 (In Russ.)

10. Rotenberg R.V. *Car suspension. Vibrations and smooth running.* M.: Mashinostroenie; 1972 (In Russ.)

11. Ablaev R.R., Chernomorets D.I. Influence of pneumatic suspension condition on stability and controllability of the vehicle. *International Journal of Humanities and Natural Sciences.* 2021;4-1(55):10–13. (In Russ.) doi: 10.24412/2500-1000-2021-4-1-10-13 EDN: UWEFHA

12. Tarasik VP. *Theory of vehicle motion.* Saint Petersburg: BHV-Peterburg; 2022. (In Russ.) EDN: FOWIQZ

13. Ageykin YaS. *Passability of automobiles.* M.: Mashinostroenie; 1981. (In Russ.)

14. Mishuta DV, Mikhailov VG. Influence of design parameters of the car and its suspension on the stability and controllability of the staff car. *Bulletin of the Belarusian-Russian University.* 2013;3(40):30–36. (In Russ.) doi: 10.53078/20778481_2013_3_30 EDN: RRYLSR

15. Safiullin RN, Kerimov MA, Valeev DH. *Design, calculation and operational properties of transport and transportation-technological machines: training manual.* St. Petersburg: Lan; 2022. (In Russ.) EDN: YIIXXP

16. Tint NV, Alakin VM. Investigation of the influence of the body roll on the transverse stability of a cargo van when turning. *Proceedings of R.E. Alekseev NSTU.* 2022;3(138):106–113. (In Russ.) doi: 10.46960/1816-210X_2022_3_106 EDN: SMGIQF

17. Krivtsov SN, Krivtsova TI, Stepanov NV. *Testing of wheeled machines: training manual.* Molodezhny: IrGAU; 2020. (In Russ.)

18. Samusenko MF. *Design and calculation of heavy-duty vehicles. Design and calculation of suspensions. Mobility and stability: training manual.* Moscow: MADI; 1984. (In Russ.)

19. Fomin VM. *Automobiles. Theory of operational properties of automobiles.* Moscow: RUDN; 2008. (In Russ.)
20. Chernyshov KV, Ryabov IM, Novikov VV, et al. *Dynamics of motion. Adjustable suspensions: training manual.* Moscow; Vologda: Infra-Inzheneriya; 2023. (In Russ.)
21. Derbaremdiker AD. *Hydraulic shock absorbers of automobiles.* M.: Mashinostroenie, 1969. (In Russ.)
22. Patent RUS for useful model № 204114/ 07.05.2021. Bull. №. 13. Artemyev V.N., Repin S.V., Dobromirov V.N., Bukirov R.R. et al. *Pneumohydraulic shock absorber.* (In Russ.) EDN: BBBIHQ
23. Safonov R.A. Typical defects of the upper road surface in Russia. *Bulletin of the South Ural State University. Series: Construction and Architecture.* 2020;20(2):75–84. (In Russ.) doi: 10.14529/build200210 EDN: WQYSOM
24. Taberlet N, Morris SW, McElwaine JN. Washboard road: the dynamics of granular ripples formed by rolling wheels. *Physical review letters.* 2007;99(6). doi: 10.1103/PhysRevLett.99.068003
25. Repin SV, Dobromirov VN, Orlov DS. Investigation of the elastic characteristic of a new pneumohydraulic shock absorber. *Bulletin of Civil Engineers.* 2019;5(76):260–269. (In Russ.) doi: 10.23968/1999-5571-2019-16-5-260-269 EDN: KIGLHH
26. Dobromirov VN, Gusev EP, Karunin MA, et al. *Shock absorbers. Design. Calculation. Testing.* Moscow: MGTU «MAMI»; 2006. (In Russ.)
27. Repin SV, Dobromirov VN, Orlov DS, et al. Investigation of Damping Characteristic of a New Hydropneumatic Shock Absorber. *Vestnik of Civil Engineers.* 2020;2(79):187–194. (In Russ.) doi: 10.23968/1999-5571-2020-17-2-187-194 EDN: MYJPDN
28. Patent RUS for useful model № 194004 / 22.11.2019. Bull. №. 33. Repin SV, Evtyukov SS, Orlov DS. *Two-tube hydropneumatic shock absorber.* (In Russ.) EDN: OTWWNB
29. Patent RUS for useful model № 208894 / 20.01.2022. Bull. №. 2. Repin SV. *Pnevmohydraulic shock absorber.* (In Russ.) EDN: SEPQCX
30. Patent RUS for useful model № 204317 / 19.05.2021. Bull. № 14. Repin SV. *Single-tube hydropneumatic shock absorber.* (In Russ.) EDN: IBGLNO
31. Patent RUS for useful model № 218675 / 05.06.2023. Bull. № 16. Bukirov RR. *Pneumohydraulic shock absorber with a remote pneumatic chamber.* (In Russ.) EDN: QUJXCP
32. Ruban VG, Matva AM. *Solution of problems of dynamics of railway crews in Mathcad package: training manual.* Rostov on Don: RGUPS; 2009. (In Russ.)
33. Rykov SP. *Fundamentals of inelastic resistance theory in pneumatic tires with applications.* St. Petersburg: Lan; 2017. (In Russ.) EDN: YTYEGM
34. Levkovsky DI, Makarov RI. *System approach to research and development of information systems.* Vladimir: VlGU; 2010. (In Russ.)
35. Volkov IV, Ruban VG. Comparative studies of the dynamic qualities of the variants of the crew part of an eight-axle electric locomotive. In: *Design and research issues of mainline and industrial electric locomotives: Collection of scientific works.* Tbilisi; 1990;55–59. (In Russ.)
36. Certificate RUS of state registration of computer program № 2024614880 / 29.02.2024. Bukirov RR. *Program of calculation of transverse static stability of transport-technological machines on a slope, taking into account the characteristics of suspension.* (In Russ.)
37. GOST 31507-2012. Motor vehicles. Steerability and stability. Technical requirements. Test methods. Introduced. 2013-10-01. Moscow: Standardinform; 2013. (In Russ.)
38. Certificate RUS of state registration of computer program № 2023683969 / 13.11.2023. Bukirov RR. *Program of calculation and estimation of energy intensity of elastic element of pneumohydraulic shock absorber with progressive elastic characteristic.* (In Russ.) EDN: HIPCSD
39. GOST 31191.1-2004. Vibration and shock. Measurement of total vibration and assessment of its effect on humans. Part 1. General requirements. Annex B. Introduced on 2018-02-01. Moscow: Standardinform, 2010. (In Russ.)
40. Shekhovtsov VV. *Podressorivanie kabinsnykh kabinsnykh i caterpillarnykh machineries.* Moscow, Vologda: Infra-Engineering; 2023 (In Russ.)
41. Technical characteristics of the tire KAMA-URAL 390/95R20. [internet]. Accessed: 16.01.2023. Available from: https://www.td-kama.com/ru/tyre_catalog/213476/

СПИСОК ЛИТЕРАТУРЫ

1. Новиков В.В., Рябов И.М., Чернышов К.В. Виброзащитные свойства подвесок автотранспортных средств. Москва, Вологда: Инфра-Инженерия, 2021. EDN: FRSPKX
2. Новиков В.В., Чернышов К.В., Поздеев А.В. и др. Комбинированные демпфирующие системы в подвесках автотранспортных средств. Москва, Вологда: Инфра-Инженерия, 2024.
3. Новиков В.В., Чернышов К.В., Поздеев А.В. Расчет систем подрессоривания автотранспортных средств: учебник. Москва; Вологда: Инфра-Инженерия, 2024.
4. Repin S.V., Bukirov R.R., Vasilieva P.V. Study on effects of damping characteristics of base chassis suspension on operational safety of transport and handling machinery // Transportation Research Procedia: 14, Saint Petersburg, 21–24 октября 2020 года. Saint Petersburg, 2020. P. 574–581. doi: 10.1016/j.trpro.2020.10.069 EDN: MTWSYH
5. Repin S., Bukirov R., Vorontsov I., et al. Improving the movement smoothness of a mobile repair shop for machinery servicing in the Arctic // Transportation Research Procedia, St. Petersburg, 02–04 июня 2021 года. St. Petersburg, 2021. P. 553–561. doi: 10.1016/j.trpro.2021.09.084 EDN: DJBMGB
6. Букиров Р.Р. Моделирование процессов демпфирования подвески транспортно-технологических средств на базе автомобильных шасси в Арктических условиях эксплуатации. В кн.: Техническое обеспечение доступности арктических регионов: Материалы III Всероссийского научного семинара, Санкт-Петербург, 27 октября 2022 года. Санкт-Петербургский государственный архитектурно-строительный университет, 2022. С. 57–65. EDN: EAMVYY
7. Дубровский А.Ф., Абрамов М.И., Сакулин Ю.А. Выбор параметров подвески грузовых автомобилей «Урал» для повышения скорости движения по изношенным грунтовым

дорогам // Вестник Оренбургского государственного университета, 2014. № 10(171). С. 66–75. EDN: TPNREB
8. Репин С.В., Масленников Н.А., Орлов Д.С., и др. Исследование процессов обеспечения плавности хода транспортно-технологических машин на базе шасси грузовых автомобилей в сложных дорожных условиях // Транспортное, горное и строительное машиностроение: наука и производство, 2023. № 23. С. 76–84. doi: 10.26160/2658-3305-2023-23-76-84 EDN: UMNUWF
9. Раймпель Й. Шасси автомобиля: Амортизаторы, шины и колеса. М.: Машиностроение, 1986.
10. Ротенберг Р.В. Подвеска автомобиля. Колебания и плавность хода. М.: Машиностроение, 1972.
11. Аблаев Р.Р., Черноморец Д.И. Влияние состояния пневматической подвески на устойчивость и управляемость транспортного средства // Международный журнал гуманитарных и естественных наук, 2021. № 4–1(55). С. 10–13. doi: 10.24412/2500-1000-2021-4-1-10-13 EDN: UWEFHA
12. Тарасик В.П. Теория движения автомобиля. Санкт-Петербург: БХВ-Петербург, 2022. EDN: FOWIQZ
13. Агейкин Я.С. Проходимость автомобилей. М.: Машиностроение, 1981.
14. Мишута Д.В., Михайлов В.Г. Влияние конструктивных параметров автомобиля и его подвески на устойчивость и управляемость штабной машины // Вестник Белорусско-Российского университета, 2013. № 3(40). С. 30–36. doi: 10.53078/20778481_2013_3_30 EDN: RRYLSR
15. Сафиуллин Р.Н., Керимов М.А., Валеев Д.Х. Конструкция, расчёт и эксплуатационные свойства транспортных и транспортно-технологических машин. Санкт-Петербург: Лань, 2022. EDN YIIXXP
16. Тинт Н.В., Алакин В.М. Исследование влияния крена кузова на поперечную устойчивость грузового фургона при повороте // Труды НГТУ им. Р.Е. Алексеева, 2022. № 3(138). С. 106–113. doi: 10.46960/1816-210X_2022_3_106 EDN: SMGIQF
17. Кривцов С.Н., Кривцова Т. И., Степанов Н.В. Испытания колёсных машин. Молодежный: ИрГАУ, 2020.
18. Самусенко М.Ф. Конструирование и расчет большегрузных транспортных средств. Конструирование и расчет подвесок. Подвижность и устойчивость. Москва: МАДИ, 1984.
19. Фомин В.М. Автомобили. Теория эксплуатационных свойств автомобилей. Москва: РУДН, 2008.
20. Чернышов К.В., Рябов И.М., Новиков В.В., и др. Динамика движения. Регулируемые подвески. Москва; Вологда: Инфа-Инженерия, 2023.
21. Дербаремдикер А.Д. Гидравлические амортизаторы автомобилей. М.: Машиностроение, 1969.
22. Патент РФ на полезную модель № 204114 / 07.05.2021. Бюл. № 13. Артемьев В.Н., Репин С.В., Добромиров В.Н., Букиров Р.Р. и др. Пневмогидравлический амортизатор. EDN: BBBIHQ
23. Сафонов Р.А. Типичные дефекты верхнего дорожного покрытия в России // Вестник Южно-Уральского государственного университета. Серия: Строительство и архитектура, 2020. Т. 20, № 2. С. 75–84. doi: 10.14529/build200210 EDN: WQYSOM
24. Taberlet, N., Morris, S.W., McElwaine, J.N. Washboard road: the dynamics of granular ripples formed by rolling wheels. Physical review letters. 2007. Vol. 99(6). doi: 10.1103/PhysRevLett.99.068003
25. Репин С.В., Добромиров В.Н., Орлов Д.С. Исследование упругой характеристики нового пневмогидравлического амортизатора // Вестник гражданских инженеров, 2019. № 5(76). С. 260–269. doi: 10.23968/1999-5571-2019-16-5-260-269 EDN: KIGLHH
26. Добромиров В.Н., Гусев Е.П., Карунин М.А., и др. Амортизаторы. Конструкция. Расчёт. Испытания. Москва: МГТУ «МАМИ», 2006.
27. Репин С.В., Добромиров В.Н., Орлов Д.С. и др. Исследование демпфирующей характеристики нового гидропневматического амортизатора // Вестник гражданских инженеров, 2020. № 2(79). С. 187–194. doi: 10.23968/1999-5571-2020-17-2-187-194 EDN: MYJPDN
28. Патент РФ на полезную модель № 194004/ 22.11.2019. Бюл. № 33. Репин С.В., Евтюков С.С., Орлов Д.С. Двухтрубный гидропневматический амортизатор. EDN: OTWWNB
29. Патент РФ на полезную модель № 208894 / 20.01.2022. Бюл. № 2. Репин С.В. Пневмогидравлический амортизатор. EDN: SEPQCX
30. Патент РФ на полезную модель № 204317/ 19.05.2021. Бюл. № 14. Репин С.В. Однотрубный гидропневматический амортизатор. EDN IBGLNO
31. Патент РФ на полезную модель № 218675/ 05.06.2023. Бюл. № 16. Букиров Р.Р. Пневмогидравлический амортизатор с выносной пневматической камерой. EDN: QUJXCP
32. Рубан В.Г., Матва А.М. Решение задач динамики железнодорожных экипажей в пакете Mathcad. Ростов-на-Дону: РГУПС, 2009.
33. Рыков С.П. Основы теории неупругого сопротивления в пневматических шинах с приложениями. Санкт-Петербург: Лань, 2017. EDN: YTYEGM
34. Левковский Д.И., Макаров Р.И. Системный подход к исследованию и разработке информационных систем. Владимир: ВлГУ, 2010.
35. Волков И.В., Рубан В.Г. Сравнительные исследования динамических качеств вариантов экипажной части восьмиосного электровоза. В кн.: Вопросы конструирования и исследования магистральных и промышленных электровозов: сб. научн. тр. Тбилиси, 1990. С. 55–59.
36. Свидетельство РФ о гос. рег. программы для ЭВМ № 2024614880 / 29.02.2024. Букиров Р.Р. Программа расчёта поперечной статической устойчивости транспортно-технологических машин на косогоре, учитывающая характеристики подвески. EDN: GDPCRR
37. ГОСТ 31507-2012. Автотранспортные средства. Управляемость и устойчивость. Технические требования. Методы испытаний. Введ. 2013-10-01. М.: Стандартинформ, 2013.
38. Свидетельство РФ о гос. рег. программы для ЭВМ № 2023683969 / 13.11.2023. Букиров Р.Р. Программа расчета и оценки энергоемкости упругого элемента пневмогидравлического амортизатора с прогрессивной упругой характеристикой. EDN: HIPCSD
39. ГОСТ 31191.1-2004. Вибрация и удар. Измерение общей вибрации и оценка её воздействия на человека. Часть 1. Общие требования. Приложение В. Введ. 2018-02-01. М.: Стандартинформ, 2010.
40. Шеховцов В.В. Подрессоривание кабин колёсных и гусеничных машин. Москва, Вологда: Инфра-инженерия, 2023.
41. Технические характеристики шины КАМА-УРАЛ 390/95R20. [iternet]. Дата обращения 16.01.2023. Режим доступа: https://www.td-kama.com/ru/tyre_catalog/213476/

AUTHOR'S INFO

Roman R. Bukirov,
Postgraduate of the Ground Transport and Technological Machines Department;
address: 4 2nd Krasnoarmeyskaya street, 190005 Saint Petersburg, Russian Federation;
ORCID: 0009-0003-9303-3142;
eLibrary SPIN: 7768-2713;
e-mail: bukirov_r.r.-king@mail.ru

ОБ АВТОРЕ

Букиров Роман Рустамович,
аспирант кафедры наземных транспортно-технологических машин;
адрес: Российская Федерация, 190005, Санкт-Петербург, 2-я Красноармейская ул., д. 4;
ORCID: 0009-0003-9303-3142;
eLibrary SPIN: 7768-2713;
e-mail: bukirov_r.r.-king@mail.ru